Dynamic Conductor Temperature Modelling and Analysis of a Distribution Network with PV

Arif Ahmed*, Fiona Stevens McFadden†, Ramesh Rayudu‡, and Tobias Massier§
*†Robinson Research Institute, *‡Smart Power and Renewable Energy Systems Group
*†‡School of Engineering and Computer Science, Victoria University of Wellington, Wellington 6140, New Zealand
*§TUMCREATE, 1 CREATE Way, #10-02 CREATE Tower, Singapore 138602
Email: *arif.ahmed@vuw.ac.nz, †fiona.stevensmcfadden@vuw.ac.nz,
‡ramesh.rayudu@vuw.ac.nz, and §tobias.massier@tum-create.edu.sg

***Abstract*—The IEEE Std 1283™-2013 details the adverse effects of high conductor temperatures, which emphasises the need to model and analyse dynamic conductor temperatures in a power network. Conductor temperatures are dependent on the power flows (due to load current), the resistive losses, and the weather conditions surrounding the conductor. Conventional power system analysis does not take into account changing weather and its impacts and as a result, studies conducted are erroneous due to absence of such realistic assumptions of the weather impacts. In this manuscript, a dynamic conductor temperature model is presented and utilised to study and thermally profile the conductor temperatures in a distribution network. The proposed approach is decoupled i.e. the power flow and the conductor heat balance model are solved separately to obtain the thermal profile network conductors in operation. In comparison to the existing approach suggested in the literature, the proposed approach is computational light and can be easily scaled to larger networks. Simulations were carried out for two cases with different load and weather conditions. The changing weather conditions and their impact on the network and thermal profile was understood by utilising the proposed technique. The simulation results presented show the advantages of using dynamic conductor temperature modelling in power system studies for better analysis of power networks.**

***Index Terms*—Dynamic Conductor Temperature Modelling, Dynamic Thermal Line Rating (DTLR), Power System Analysis, Thermal Profiling of Conductors**

I. Introduction

Evolution of power systems into modern smart grids and advancements in microgrid technologies have brought about drastic changes to how power systems are perceived today [1]. As power systems evolve into complex modern systems, accurate modelling becomes crucial in understanding and analysing them.

Conventional power system studies neglect the effect of weather conditions, which affects power system analysis [2]–[7] by impacting power system states and network characteristics (temperature and resistance of the network conductors). Power lines are the backbone of any power system and must always be operated under safe temperature limits. The conductor temperature in a power network is affected by the current flow, the resistive losses, and the surrounding weather conditions. Weather conditions affect the power transfer capability of power lines by impacting the conductor temperature and resistance [8], [9]. Authors of [7] showed that significant differences in power flow analysis are observable when changing weather conditions are considered, which can improve the accuracy of power flow analysis. The power loss error between conventional power flow (PF) calculations and the temperature and resistance corrected power flow (based on weather conditions) calculations could reach up to $30\,\%$ and this error varies with the changing weather and load conditions [2]. It is reported in [10] that the use of accurate conductor temperature and resistance allows accurate allocation of power losses and more accurate determination of the power flows and network voltage profiles. The study in [6] presented the effects of weather conditions on transient stability by considering various conductors and highlighted the importance of weather conditions in power system transient stability studies. All the aforementioned studies indicate the importance of considering weather conditions to improve power system studies, which can be achieved by appropriately modelling power systems by incorporating information of weather conditions.

Varying weather conditions relate to the variation of temperature profiles of power lines which is amongst the most important factors related to the structural decay of power lines [11]. Therefore, in [11], authors evaluated the effect of progressive wire rupture on the temperature profile of Aluminium Conductor Steel Reinforced (ACSR). In addition, conductors sustaining high temperatures due to weather conditions are subject to loss in tensile strength and current carrying capacity leading to increased sag and decreased ground clearance [12]–[14]. This increases the risk of operational safety. Furthermore, high operating temperatures reduce the useful life of conductors, accelerate ageing, and increase the resistive losses. Therefore, monitoring and thermal profiling of the conductor temperature is crucial in safe, secure, and reliable power system operation.

Information on weather conditions and conductor temperature is also important for Dynamic Thermal Line Rating (DTLR), i.e., the maximum allowable conductor current carrying capacity under any given weather condition. In comparison to traditional static line ratings, DTLR allows more flexibility to system operators by allowing active management power networks. DTLR also aids utilities by deferring investments in line upgrade or installation of new lines [15].

Numerous studies in the literature focus on evaluating the steady-state conductor temperature of power networks through power flow analysis [2], [4], [5], [7], [16], etc. utilising weather information. However, conductor temperature of power conductors change dynamically and not instantaneously due to the heat capacity of the conductor material, which is attributed as the thermal inertia of the conductor. It is, therefore, important to model and analyse the dynamic conductor temperature of conductors in operation for a more accurate and beneficial analysis.

Authors in [5] proposed a PFA by time-domain simulation of the non-steady-state nonlinear heat balance model of the IEEE Std 738™-2012 [8]. Conventional power flow algorithm is sequentially coupled with the time-domain simulation of the heat balance model in [5] and is solved iteratively to calculate accurate power flow that incorporates weather conditions. As a result, the technique yields good accuracy but is computationally costly due to the coupled time-domain simulation of differential equations. In fact, the authors simulated the IEEE 39-bus New England Test System for an hour of simulation time with a step-size of $0.01\,\mathrm{s}$ that took $414.13\,\mathrm{s}$ on average. This indicates that simulation of large networks with high resolution weather data is computationally very challenging requiring longer computation time and as a result, scalability of application is of concern.

Therefore, in this manuscript, we model and analyse the dynamic conductor temperature of line conductors for a distribution network by proposing a computationally light technique. The method presented is aimed at generating approximate thermal profile of conductors in operation to aid power system studies. This will aid in improving subsequent power system analyses like planning, design, control, operation, and expansion of power grids.

The contributions of this manuscript are as follows:

1) A computationally light technique to estimate the dynamic conductor temperature utilising the non-steady-state nonlinear heat balance model recommended by IEEE Std 738™-2012 [8] that follows from the conventional power flow.
2) Improved understanding of network impacts and conductor temperature profiles by simulation and analysis of a 12-bus distribution network under two distinct cases.

To achieve this, the network was simulated with and without photovoltaic (PV) systems and real weather data was utilised. Furthermore, the contributions are also supplemented by a month-long time-domain simulation of the heat balance model of branch conductors to thermally profile the conductors under the influence of weather conditions.

Section II of the manuscript presents the non-steady-state nonlinear heat balance model utilised and a flowchart of the simulation methodology undertaken. Section III discusses the 12-bus single-phase AC distribution network model studied in this manuscript. Simulation results are presented and discussed in Section IV and the manuscript is concluded in Section V.

II. Dynamic Conductor Temperature Modelling

IEEE Std 738™-2012 [8] deals with the electro-thermal relationship of overhead conductors. It is based on a modified method of House and Tuttle [17]. In this manuscript, the non-steady-state nonlinear heat balance model utilised in the IEEE Std 738™-2012 [17] is considered and modelled in MATLAB® Simulink® to study the dynamic conductor temperature states.

A conductor's temperature is a nonlinear function of multiple parameters and variables defined as follows:

$$T_c = f(m, C_p, R, T_{\text{ambient}}, \alpha, Q_s, D, H_e, V_s, W_{\text{angle}}, \epsilon, I), \quad (1)$$

with

m	mass per unit length $(\mathrm{kg/m})$
C_p	specific heat of the conductor material $(\mathrm{J/(kg\,^\circ C)})$
R	conductor resistance per unit length (Ω/m)
T_{ambient}	ambient temperature $(^\circ\mathrm{C})$
α	solar absorptivity
Q_s	global solar irradiance $(\mathrm{W/m^2})$
D	conductor diameter (m)
H_e	conductor elevation above sea level (m)
V_s	wind speed $(\mathrm{m/s})$
W_{angle}	wind incidence angle or direction $(^\circ)$
ϵ	emissivity of the conductor
I	current flowing in the conductor (A)

The differential heat balance equation of a conductor can be simplified for the dynamic temperature of a conductor [8], [18] as follows:

$$\frac{dT_c}{dt} = \frac{1}{mC_p}[I^2 R(T_c) + q_s - q_c - q_r] \quad (2)$$

In Equation (2), $R(T_c)$ is the resistance of the conductor at the conductor temperature T_c. It can be calculated as [8]:

$$R(T_c) = \left[\frac{R(T_{\text{high}}) - R(T_{\text{low}})}{T_{\text{high}} - T_{\text{low}}}\right](T_c - T_{\text{low}}) + R(T_{\text{low}}) \quad (3)$$

Here, $R(T_{\text{high}})$ is the conductor resistance at a higher temperature while $R(T_{\text{low}})$ is the conductor temperature at a lower temperature ($T_{\text{high}} > T_{\text{low}}$). The solar heat gain rate is denoted by q_s, while q_c is the convective heat loss rate and q_r is the radiated heat loss rate (all given in $\mathrm{W/m}$).

The solar heat gain rate of a conductor depends on its diameter (D), the absorptivity (α), and the global solar irradiance (Q_s) [9]. This relationship is presented in Equation (4).

$$q_s = \alpha Q_s D \quad (4)$$

The convective heat loss rate (q_c) of a conductor is of two types [8], [9]: natural convection and forced convection. The following equations can be utilised to calculate the convective heat loss rate.

$$\begin{aligned} q_{c_1} &= K_{\text{angle}}[1.01 + 1.35{N_{\text{Re}}}^{0.52}]k_f(T_c - T_{\text{ambient}}) \\ q_{c_2} &= 0.754 K_{\text{angle}} {N_{\text{Re}}}^{0.6} k_f(T_c - T_{\text{ambient}}) \\ q_{c_n} &= 3.645 {\rho_f}^{0.5} D^{0.75}(T_c - T_{\text{ambient}})^{1.25} \end{aligned} \quad (5)$$

$$\frac{dT_c}{dt} = \frac{1}{mC_p}\left[I^2\left[\left(\frac{R(T_{\text{high}})-R(T_{\text{low}})}{T_{\text{high}}-T_{\text{low}}}\right)(T_c - T_{\text{low}}) + R(T_{\text{low}})\right] + \alpha Q_s D - K_{\text{angle}}[1.01 + 1.35{N_{\text{Re}}}^{0.52}]k_f(T_c - T_{\text{ambient}}) - \pi\sigma_B\epsilon D[(T'_c)^4 - (T'_{\text{ambient}})^4]\right] \tag{7}$$

In Equation (5), q_{c_1} and q_{c_2} represent forced convection, while natural convection is represented by q_{c_n}. IEEE Std 738™-2012 recommends using the largest calculated value of q_{c_1}, q_{c_2}, and q_{c_n} for the convective heat loss rate at any given weather condition. K_{angle} is the wind direction factor, N_{Re} is the Reynolds number, k_f is the thermal conductivity of air, and ρ_f is the air density. Detailed equations can be referred to in the IEEE Std 738™-2012.

The radiated heat loss rate q_r represents the rate at which the heat energy of a conductor is radiated to its surroundings. The equation to calculate the radiated heat loss rate [8] is given as:

$$q_r = \pi\sigma_B\epsilon D[(T'_c)^4 - (T'_{\text{ambient}})^4] \tag{6}$$

with σ_B being the Stefan-Boltzmann constant and T'_c, T'_{ambient} the temperatures in Kelvin.

The dynamic conductor temperature state of a conductor under changing weather and load conditions can be calculated by substitution of Equations (2)–(6) in Equation (1) and solving the resulting differential equation (presented by Equation (7)). It should be noted that in Equation (7), q_{c_1} is substituted for the expression of q_c. However, as mentioned earlier, the expression that yields the largest convective heat rate should be selected.

In this manuscript, individual network conductors are modelled with the differential equation in MATLAB® Simulink®. The model takes m, C_p, R, T_{ambient}, α, Q_s, D, H_e, V_s, W_{angle}, ϵ, and I as inputs to output the dynamic conductor temperature T_c.

A. Flowchart representation of the simulation methodology

As mentioned in Section I, the time-domain simulation methodology presented in [5] is computationally complex and as a result a computationally light approach is undertaken in this manuscript, which is decoupled in terms of the solution of power flow and the non-steady-state heat balance model. A flowchart of the methodology is presented in Figure 1.

As represented in Figure 1, a steady-state time-series power flow is first executed for all the given data, which is then followed by the time-domain simulation of the heat balance model of the branch conductors. The time-domain simulation of the heat balance utilises the conductor currents solved from the power flow and the weather conditions as depicted in Figure 1. From the time-domain simulation, the thermal profiles and the dynamic resistance of the conductors are obtained, which are then utilised to calculate the temperature-corrected power losses.

III. Network Modelling

A 12-bus single-phase AC distribution network with two $5\,\text{kW}_\text{p}$ solar systems is modelled for the purpose of the simulation study as shown in Figure 2. Every individual branch

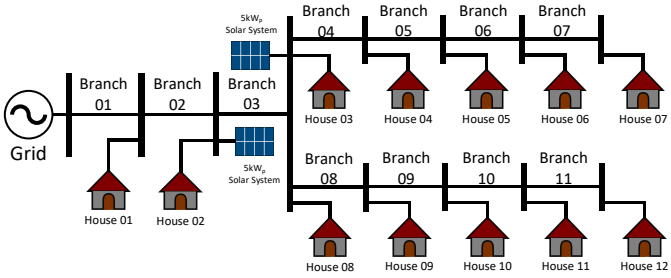

Fig. 2: 12-house single-phase distribution network.

is considered to be of $10\,\text{m}$ in length and made of 795 kcmil ACSR [8] conductor. Thus, the resistance of a single branch is $7.283 \times 10^{-4}\,\Omega$ at $25\,^\circ\text{C}$, while the inductance is $8.943 \times 10^{-6}\,\text{H}$. The line capacitance is negligible. The pole configuration is shown in Figure 3. The network is operated at $230\,\text{V}_\text{rms}$ $50\,\text{Hz}$ and the grid is considered a slack node. All the houses are modelled as PQ [19] node with an inductive load power factor. The solar systems are also modelled as PQ node with unity power factor injection. Both the network and the heat balance models are developed in MATLAB® Simulink® and simulation studies were performed.

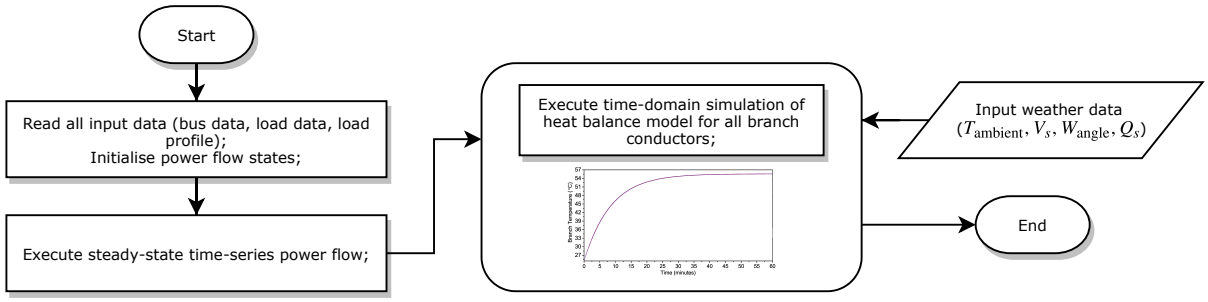

Fig. 1: Flowchart representation of simulation methodology for thermal profiling.

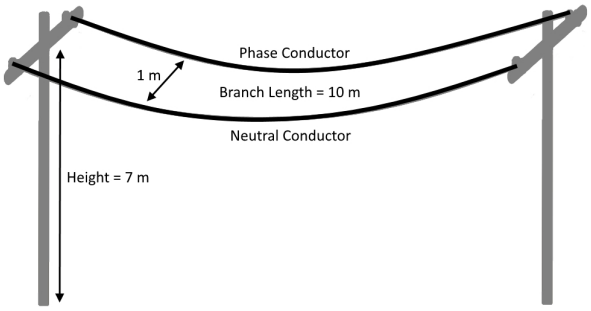

Fig. 3: Distribution pole and line configuration.

IV. Simulation Results and Discussion

For the study, two cases were simulated and analysed. In Case 1, the impact of PV on the dynamic conductor temperature state of the network was investigated. This was achieved by first simulating all houses at their peak load under a considered weather condition for an hour with no PV systems connected. The same case was then repeated with the PV systems connected, generating a peak output of 5 kW each.

For Case 2, all the loads were fixed at their peaks with the PV systems disconnected while the weather conditions varied throughout a month according to the data collected [20]. Weather data of 10-min resolution comprising ambient temperature, global solar irradiance, wind speed and wind direction/angle was collected and filtered from a weather station in the North Island of New Zealand for January 2016 [20]. Effectively, this case illustrates the effect of weather conditions on the dynamic conductor temperature state of the network.

A. Case 1

The peak load data for Case 1 is presented in Table I and the weather-related data is presented in Table II.

TABLE I: Load data for Case 1. A negative value of P indicates power injection.

	P (kW)	Q (kVAR)	Power Factor
Houses 01–07	13.5	6.538	0.9
Houses 08–12	18.0	8.717	0.9
Solar Systems 01–02	−5.0	0	1.0

TABLE II: Simulation Data.

Parameter/Variable	Value
m (aluminium)	$1.116\,\mathrm{kg/m}$
m (steel)	$0.5119\,\mathrm{kg/m}$
C_p (aluminium)	$995\,\mathrm{J/(kg\,°C)}$
C_p (steel)	$476\,\mathrm{J/(kg\,°C)}$
R at 25 °C	$72.83\,\mu\Omega/\mathrm{m}$
T_{ambient}	25 °C
α	0.8
Q_s	$1000\,\mathrm{W/m^2}$
D	0.0281 m
H_e	7 m
V_s	2 m/s
W_{angle}	45°
ϵ	0.8

The dynamic conductor temperature state of the branches for Case 1 is presented in Figure 4. It can be observed that branches 01 to 03 have higher temperatures without PV systems connected. This is due to higher current flow from the source side to meet the load demand. The branch temperatures of the heavily loaded branches decrease noticeably when PV systems are connected to the network. As the PV systems inject power into the network, the grid has to supply less power as compared to no PV systems being connected. This in turn leads to lower branch conductor temperature.

The resistance of a conductor is related to its temperature as shown in Equation (3). The change in conductor temperature yields change in the resistance of the conductors in operation, which is presented in Figure 5. It is observed that the branch resistance follows the branch conductor temperature.

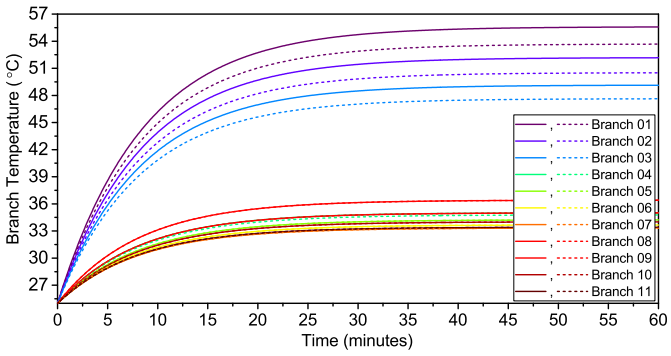

Fig. 4: Conductor temperature of the branches (Case 1). Dotted lines represent branch temperatures with PV systems while solid lines represent branch temperatures without PV systems.

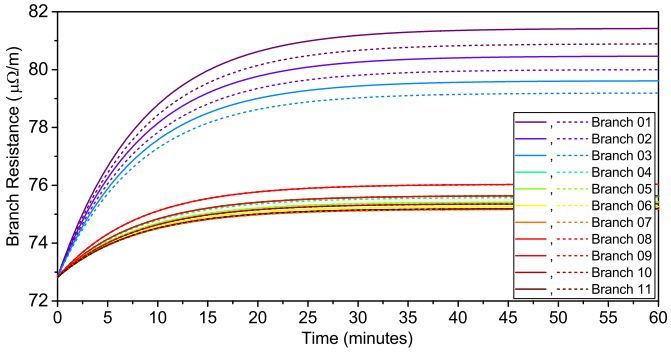

Fig. 5: Conductor resistance of the branches: Case 1. Dotted lines represent branch resistance with PV systems while solid lines represent without PV systems.

Table III presents important results from the simulation, including branch currents, branch power losses, and branch loadings; once with and once without connected PV systems. For the simulated case, the DTLR was calculated to be 1428.91 A at the given weather conditions. The branch loadings were calculated based on the DTLR. Since the entire network is assumed to be operating under the same weather

conditions with the same branch conductors, the DTLRs of all branches are the same.

In Table III, it can be seen that the branch currents of the highly loaded branches decreased with connected PV systems. This also lead to reduced branch power losses, reduced branch loadings, and reduced branch temperatures.

TABLE III: Branch current, power loss, and loading (Case 1).

Branch No.	Branch current (A)		Power loss (W)		Branch loading (%)	
	No PV	PV	No PV	PV	No PV	PV
01	874.05	838.31	545.09	504.83	61.17	58.67
02	808.60	774.12	467.19	429.89	56.59	54.17
03	744.17	709.74	395.73	361.38	52.08	49.67
04	255.10	237.96	46.50	40.63	17.85	16.65
05	191.20	191.19	26.13	26.21	13.38	13.38
06	127.41	127.40	11.60	11.64	8.92	8.92
07	63.69	63.68	2.90	2.91	4.46	4.46
08	339.67	339.62	82.46	82.72	23.77	23.77
09	254.54	254.62	46.31	46.45	17.81	17.81
10	169.60	169.57	20.56	20.62	11.87	11.87
11	84.77	84.75	5.14	5.15	5.93	5.93

B. Case 2

In Case 2, all loads were considered to be fixed at their peaks and the weather conditions were assumed to vary throughout the month. The dynamic conductor temperature of the branches for Case 2 is presented in Figure 6. As the weather conditions vary throughout the month, significant variation in the branch temperatures is observed in Figure 6. The highly loaded branches 01 to 03 get closer to their thermal limits of $100\,^{\circ}\mathrm{C}$ [8] numerous times throughout the month. This indicates that these branches experience more thermal stress than the rest of the network, resulting in earlier ageing and deterioration. A zoomed-in view of the conductor temperatures from day 7 to 8 is presented in Figure 6. The month-long time-domain simulation of the heat balance model of the 11 branch conductors in Case 2 took less than $8\,\mathrm{s}$ on a standard desktop computer.

The minimum, maximum, range, and standard deviation of the branch temperatures are presented in Table IV. It is observed that the highly loaded branches are noticeably affected by the changing weather yielding higher minimum, maximum, range, mean, and standard deviation in branch temperature.

TABLE IV: Minimum, maximum, range, mean, and standard deviation of branch temperatures for Case 2.

Branch No.	Min (°C)	Max (°C)	Range (°C)	Mean (°C)	Standard deviation (°C)
01	14.51	95.63	81.12	30.23	9.52
02	13.81	86.49	72.67	28.45	8.33
03	13.18	78.15	64.97	26.84	7.33
04	7.39	45.83	38.44	19.30	4.84
05	6.50	44.12	37.62	18.88	4.87
06	5.81	42.87	37.06	18.58	4.91
07	5.41	42.14	36.74	18.40	4.93
08	8.96	48.90	39.94	20.05	4.84
09	7.38	45.81	38.43	19.30	4.84
10	6.23	43.63	37.40	18.76	4.88
11	5.51	42.33	36.82	18.44	4.92

C. Discussion

The simulation study and results presented show the advantages of dynamic conductor temperature modelling and analysis in power networks. As shown in the simulation cases, dynamic conductor modelling and analysis could be utilised to understand the nature of the conductor temperatures in an operational environment. This will help in thermal profiling of the conductors and estimating ageing and deterioration. It will also aid in real-time active network management by understanding the loaded nature of conductors and the margins available to push more power through them. In real-time operation, loads, currents, and environmental conditions are always changing. This changing nature and its effect on the network can be understood by the presented modelling and analysis approach.

In the undertaken case studies, it has been observed that the impact of changing weather on the dynamic temperature state of conductors increases with higher loading of the branch conductors. Furthermore, integration of Distributed Energy Resources (DER), e.g., PV systems, can help improve the thermal profile of operating conductors in a network as observed from the simulation. It is also understood that ideally, DER should be placed near highly loaded branches to improve the thermal profile of the network. Due to the observed changes in branch loadings and power losses resulting from changing weather conditions, changes in power system states are expected. As a consequence, dynamic conductor temperature modelling could prove to be important for approximating the thermal profiles of large networks and aid in planning, design, and operation analysis of power networks.

V. Conclusion

The dynamic conductor temperature modelling and analysis performed in this manuscript presents a novel perspective to traditional power network analysis which will benefit power system studies. The methodology presented utilises the non-linear heat balance of IEEE Std 738$^{\mathrm{TM}}$-2012 which takes into account weather conditions, conductor characteristics, and current to output the dynamic conductor temperature, dynamic resistance, and DTLR. The simulation methodology is computationally light and therefore can be utilised to study larger power networks. Two cases were simulated and presented to highlight the benefit of the proposed approach in power system studies. Future work entails looking at networks with multiple conductor types and scenarios as well as exploration of the applications in various power system studies. Also, since decoupled analysis was performed, investigation of error in comparison to a coupled time-domain analysis is also expected.

Acknowledgment

This work was financially supported by the Singapore National Research Foundation under its Campus for Research Excellence And Technological Enterprise (CREATE) programme.

References

[1] C. Liu, S. McArthur, and S. Lee, *Smart Grid Handbook*. Wiley, 2016.

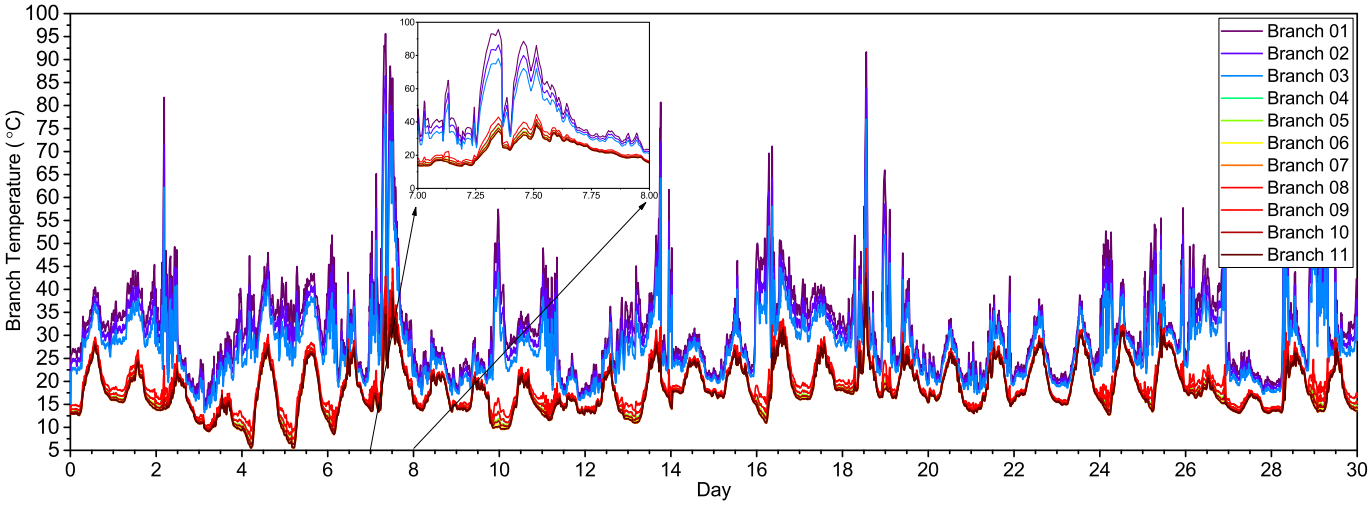

Fig. 6: Dynamic conductor temperature of the branches due to a month-long weather data consideration: Case 2.

[2] J. R. Santos, A. G. Exposito, and F. P. Sanchez, "Assessment of conductor thermal models for grid studies," *IET Generation, Transmission Distribution*, vol. 1, no. 1, pp. 155–161, Jan. 2007.

[3] S. Frank, J. Sexauer, and S. Mohagheghi, "Temperature-dependent power flow," *IEEE Transactions on Power Systems*, vol. 28, no. 4, pp. 4007–4018, Nov. 2013.

[4] A. Ahmed, F. S. McFadden, and R. Rayudu, "Impacts of distributed PV in a smart grid using temperature-dependent power flow," in *2017 IEEE Innovative Smart Grid Technologies - Asia (ISGT-Asia)*, Dec. 2017.

[5] A. Kubis and C. Rehtanz, "Application of a combined electro-thermal overhead line model in power flow and time-domain power system simulations," *IET Generation, Transmission & Distribution*, vol. 11, no. 8, pp. 2041–2049, 2017.

[6] A. Ahmed, F. S. McFadden, and R. Rayudu, "Transient stability study incorporating weather effects on conductors," in *2018 IEEE Power and Energy Society General Meeting (PESGM)*, Aug. 2018.

[7] A. Ahmed, F. J. Stevens McFadden, and R. K. Rayudu, "Weather-dependent power flow algorithm for accurate power system analysis under variable weather conditions," *IEEE Transactions on Power Systems*, pp. 1–1, 2019.

[8] "IEEE standard for calculating the current-temperature relationship of bare overhead conductors," *IEEE Std 738-2012 (Revision of IEEE Std 738-2006 - Incorporates IEEE Std 738-2012 Cor 1-2013)*, pp. 1–72, Dec. 2013.

[9] CIGRE Working Group 22.12, "Thermal behaviour of overhead conductors," *Technical Brochure 207*, 2002.

[10] M. Bockarjova and G. Andersson, "Transmission line conductor temperature impact on state estimation accuracy," in *2007 IEEE Lausanne Power Tech*, July 2007, pp. 701–706.

[11] C. A. Cimini and B. Q. A. Fonseca, "Temperature profile of progressive damaged overhead electrical conductors," *International Journal of Electrical Power & Energy Systems*, vol. 49, pp. 280–286, 2013.

[12] "IEEE guide for determining the effects of high-temperature operation on conductors, connectors, and accessories," *IEEE Std 1283-2013 (Revision of IEEE Std 1283-2004)*, pp. 1–47, Oct 2013.

[13] V. T. Morgan, "The loss of tensile strength of hard-drawn conductors by annealing in service," *IEEE Transactions on Power Apparatus and Systems*, vol. PAS-98, no. 3, pp. 700–709, May 1979.

[14] F. Jakl and A. Jakl, "Effect of elevated temperatures on mechanical properties of overhead conductors under steady state and short-circuit conditions," *IEEE Transactions on Power Delivery*, vol. 15, no. 1, pp. 242–246, 2000.

[15] S. Karimi, P. Musilek, and A. M. Knight, "Dynamic thermal rating of transmission lines: A review," *Renewable and Sustainable Energy Reviews*, vol. 91, pp. 600–612, 2018.

[16] V. Cecchi, A. S. Leger, K. Miu, and C. O. Nwankpa, "Incorporating temperature variations into transmission-line models," *IEEE Transactions on Power Delivery*, vol. 26, no. 4, pp. 2189–2196, Oct 2011.

[17] K. E. House and P. D. Tuttle, "Current-carrying capacity of ACSR," *Electrical Engineering*, vol. 77, no. 8, pp. 719–719, Aug. 1958.

[18] R. Stephen, G. Pirovano, M. Tunstall, Y. Ojala, A. McCulloch, F. Jakl, K. Bakic, L. Varga, T. Seppa, H. Pohlman *et al.*, "The thermal behaviour of overhead conductors sections 1 and 2 mathematical model for evaluation of conductor temperature in the steady state and applications thereof," *Electra*, no. 144, pp. 107–125, 1992.

[19] J. Glover, M. Sarma, and T. Overbye, *Power System Analysis and Design*. Cengage Learning, 2011.

[20] "CliFlo: NIWA's National Climate Database on the Web," http://cliflo.niwa.co.nz/, Retrieved Feb. 2017.